

Roughness of ice shelves is correlated with basal melt rates

Ray H Watkins¹, Jeremy N. Bassis¹, and M. D. Thouless¹

¹University of Michigan-Ann Arbor

November 23, 2022

Abstract

Ice shelf collapse could trigger widespread retreat of marine-based portions of the Antarctic ice sheet. However, little is known about the processes that control the stability of ice shelves. Recent observations have revealed that ice shelves have topographic features that span a spectrum of wavelengths, including basal channels and crevasses. Here we use ground-penetrating radar data to quantify patterns of roughness within and between ice shelves. We find that roughness follows a power-law with scaling exponent approximately constant between ice shelves. However, the magnitude of roughness varies by over an order of magnitude between different ice shelves. Critically, we find that roughness strongly correlates with basal melt rate, suggesting that increased basal melt not only leads to deeper melt channels, but also increased fracturing, rifting and de-creased ice shelf stability. This hints that the mechanical stability of ice shelves may be more tightly controlled by ocean forcing than previously thought.

Roughness of ice shelves is correlated with basal melt rates

Ray H. Watkins¹, Jeremy N. Bassis², and M. D. Thouless¹

¹Department of Materials Science and Engineering, University of Michigan

²Department of Climate and Space Sciences and Engineering, University of Michigan

^{1,2}Ann Arbor, MI, USA

Key Points:

- Ice shelves have bumps in their topography that correspond to crevasses, melt channels and other features
- We quantify the size of these bumps, called roughness, and find that the magnitude is spatially variable both between and within ice shelves
- Roughness of different ice shelves strongly correlates with the magnitude of basal melt

Corresponding author: Ray H. Watkins, rayhw@umich.edu

Abstract

Ice shelf collapse could trigger widespread retreat of marine-based portions of the Antarctic ice sheet. However, little is known about the processes that control the stability of ice shelves. Recent observations have revealed that ice shelves have topographic features that span a spectrum of wavelengths, including basal channels and crevasses. Here we use ground-penetrating radar data to quantify patterns of roughness within and between ice shelves. We find that roughness follows a power-law with scaling exponent approximately constant between ice shelves. However, the magnitude of roughness varies by over an order of magnitude between different ice shelves. Critically, we find that roughness strongly correlates with basal melt rate, suggesting that increased basal melt not only leads to deeper melt channels, but also increased fracturing, rifting and decreased ice shelf stability. This hints that the mechanical stability of ice shelves may be more tightly controlled by ocean forcing than previously thought.

Plain-Language Summary

The future stability of the Antarctic ice sheet is linked to the stability of floating portions of the ice sheet called ice shelves. There has been recent speculation that the collapse of ice shelves could trigger an acceleration of the discharge of grounded ice, resulting in an accelerated sea level rise. Recent observations show that the topography of ice shelves is related to features, such as melt channels and crevasses, that are a direct result of melting and fracturing. Here we use ground-penetrating data collected from various field campaigns to calculate roughness of seven ice shelves across Antarctica. We find that roughness varies considerably between ice shelves and that increased roughness strongly correlates with increased basal melt. This connection hints at a complex interplay between increased melt rates and roughening of ice shelves, and suggests that basal melt may trigger widespread fracturing, influencing the mechanical stability of ice shelves.

1 Introduction

Ice shelves—slabs of floating ice fed by flow from the grounded ice upstream—play a critical role limiting the discharge of grounded ice from the Antarctic ice sheet into the ocean (Dupont & Alley, 2005; Pritchard et al., 2012; Gudmundsson, 2013; Shepherd et al., 2018). Because ice shelves are in contact with both the ocean and atmosphere, they are sensitive to atmospheric and oceanic warming. For example, the explosive melt-water related disintegration of the Larsen A and B ice shelves in 1995 and 2002, provide a vivid illustration of the speed with which ice shelves can disintegrate (Rott et al., 1996; Scambos et al., 2003; Robel & Banwell, 2019). Both of these events coincided with increased ice discharged into the ocean (Rignot, 2004; Rignot et al., 2019), linking the demise of ice shelves directly with increased mass flux, and increased rise in global sea levels.

Although rising atmospheric temperatures are responsible for the melt-water driven collapse of sections of the Larsen ice shelf, the temperatures in many other parts of Antarctica, like the Amundsen Sea Embayment, remain cold and there is little sustained surface melting (Dixon, 2007; Werner et al., 2018). Instead, thinning, grounding line retreat and the instability of these glaciers is connected with basal melt associated with the intrusion of warm ocean waters (Jenkins et al., 2018; Nakayama et al., 2019). Recent observations and simulations show that in addition to eroding contact with the margins and pinning points, basal melt can sculpt complex and heterogeneous basal channels (Dutrieux et al., 2014; Nakayama et al., 2019). Similarly, deep basal crevasses that eventually penetrate the entire ice thickness and become rifts have also been observed across many ice shelves (McGrath et al., 2012; Jeong et al., 2016).

Rifts, crevasses and melt channels contribute to the overall topography and roughness of ice shelves. However, the connection—if any—between the processes responsible for these features remains poorly understood. One possibility is that increased basal melt results in decreased ice thickness, reducing the restraining lateral shear stresses and, potentially, allowing the ice shelf to become un-moored from pinning points (Still et al., 2018). This

reduction in restraining forces could thus result in increased fracturing and decreased mechanical stability (Favier et al., 2016). Thus, one hypothesis is that increased ocean forcing results in thinning, reducing buttressing and increasing crevassing and rifting. Similarly, formation of melt channels can alter the stress distribution within the ice, promoting basal and surface fracture and/or excavating existing basal crevasses (Vaughan et al., 2012; Bassis & Ma, 2015; Alley et al., 2016). This suggests the complementary hypothesis that ocean forcing may also directly increase fracture and failure of ice shelves through the formation of melt channels and/or excavation of basal crevasses. Here, we use existing ground-penetrating radar measurements to characterize roughness of ice shelves and the relationship between roughness and basal melt for a suite of Antarctic ice shelves.

2 Methods

2.1 Data and Study Regions

We used ground-penetrating radar data from a variety of sources (Table 1) to determine the thickness of ice shelves. All available data that covers the Pine Island, Ross, Thwaites, Dotson, Getz, Larsen C, and Filchner ice shelves were used. These ice shelves were chosen because multiple tracks covered the region, and because these regions provide contrasting environmental and glaciological conditions. For instance, the Pine Island and Thwaites ice shelves are subject to significant basal melting (Webber et al., 2017; Jenkins et al., 2018), whereas the Ross ice shelf is subject to colder ocean conditions and much lower melt rates (Dixon, 2007; Liu et al., 2015).

We performed a more detailed study of Pine Island and Ross because of the abundant data coverage for these two ice shelves, and because of the contrasting climatological forcing. For instance, Pine Island is subject to large basal melt rates along the grounding line that can exceed hundreds of meters per year (Dutrieux et al., 2013; Shean et al., 2019), resulting in an elevated average basal melt across the entire ice shelf (Liu et al., 2015). The increased melt rate has triggered grounding line retreat (Favier et al., 2014) and, potentially, increased iceberg calving (Liu et al., 2015). By con-

trast, the Ross ice shelf experiences much lower basal melt rates (Bell et al., 2020), with stable grounding line positions.

Data Name	Data Source	Reference
MCoRDS L2 Ice Thickness	Operation IceBridge	(Paden et al., 2010)
Pine Island Ice Shelf 2011	Geophysics Data Portal	(Vaughan et al., 2012)
Total Ice Thickness	ROSSETTA-Ice	(Bell et al., 2020)
Average Basal Melt	Multiple Sources	(Liu et al., 2015)

Table 1. List of data products used in this study.

2.2 Quantifying roughness

We followed (Whitehouse, 2004), and defined roughness (in meters) as the square root of the integral of the power spectral density $S(k)$:

$$R = \sqrt{\int_{k_1}^{k_2} S(k) dk}, \quad (1)$$

where k (1/m) represents the wavenumber, and k_1 (1/m), k_2 (1/m) represent the range of integration in wavenumber space. The range is related to the resolution of the data and length of tracks analyzed.

To calculate spatial variations in roughness across individual ice shelves, we first computed power spectra at windowed distances of size w , set to 3000 m, and overlap percentage m , set to 99 %. Roughness was then obtained through numerical integration of equation 1 along each of the windows. Traditionally, the Fourier transform is used to estimate the power spectral density. However, we instead used a continuous wavelet transform which produces improved along-track resolution by providing optimal basis functions that avoid spectral leakage when windowing the data (Sifuzzaman, 2009). This allowed us to resolve spatial variations in roughness at higher resolution.

We also computed the average roughness for each ice shelf by first computing the average power spectral density (obtained by averaging the spec-

tra of all tracks), and then numerically integrating to find the average roughness. This approach has the advantage that it also provided an average spectrum for each ice shelf. We chose integration bounds between 100 (1/m) for k_1 and 20000 (1/m) for k_2 so that we could consistently compare roughness between ice shelves of different dimensions. Our results are not sensitive to any windowing or scaling parameters when the parameters are varied over an order of magnitude. Moreover, we experimented with computing roughness and average roughness using a range of definitions, including just taking the mean of the windowed roughness measurements. Different definitions can influence the magnitude of roughness, but the trends and relative values are insensitive to any change in the definition of roughness used.

2.3 Spectral characteristics of roughness

If the power spectral density has peaks associated with features that have specific wavelengths, we can identify the dominant wavelength (or wavenumber) from the power spectra. Alternatively, the topography of many surfaces on Earth, Mars and Venus are power-law over a range of wavelengths (Lovejoy, 1982; Mandelbrot & Wheeler, 1983). If the topography follows a power-law distribution, the power spectral density, takes the form:

$$PSD(k) = S(k) = Ck^{-\alpha}, \quad (2)$$

where C is a roughness scaling parameter, α is the power-law (or fractal) exponent, and k (1/m) is the wavenumber. The exponent α is commonly represented as the fractal dimension F_D (Joe et al., 2017), with the relationship between α and F_D expressed by $F_D = \frac{-\alpha+8}{2}$.

We first followed (Clauset et al., 2009) to estimate if the power spectral density could be described as a power-law. We then estimated the scaling exponent α , including a minimum cutoff frequency into the fit of the exponent (Clauset et al., 2009) to account for limits in the resolution of our data. After estimating the exponent, we determined C by performing a least-squares regression to the power-law.

3 Results

3.1 Roughness of the Pine Island and Ross ice shelves

We first examined roughness of the Pine Island and Ross ice shelves. Roughness of Pine Island (Figure 1a) varies from close to ~ 0 m in the central portions and near the calving front to around ~ 60 m near the grounding line and pinning points. We see larger roughness in isolated regions of the ice shelf, corresponding to topographic features like pinning points (box A), melt channels (box B), crevasses in shear margins (box C), and rifts (box D). These structural features have all been previously documented in the ice shelf (Haran et al., 2014; Vaughan et al., 2012). Pine Island may have retreated off the pinning point (box A) between 2009 and 2011 (Favier et al., 2014), and the elevated roughness may be a legacy of previous episodic grounding on and/or processes associated with un-mooring from the pinning point.

By contrast, roughness of the Ross ice shelf (Figure 1b) is much lower overall compared to Pine Island, with values rarely exceeding 10 m and it is less than 3 m on the majority of the ice shelf. Despite the smaller overall roughness of the Ross ice shelf, we still see elevated roughness relative to the mean for both ice shelves around pinning points, melt channels, shear margins and rifts (Figure 2). All of these structures create a topographic signature in roughness, but the magnitude varies substantially between ice shelves.

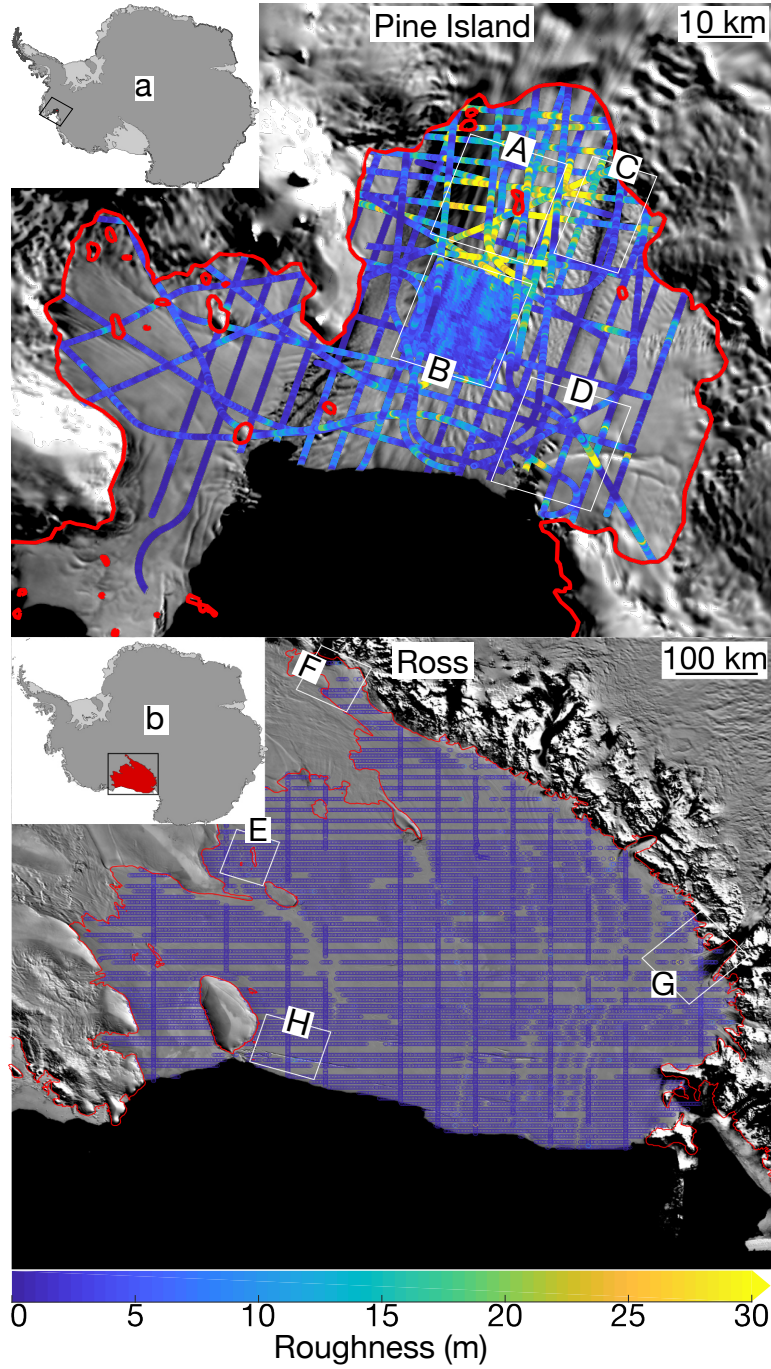


Figure 1. Spatial patterns of roughness for a) the Pine Island ice shelf and b) the Ross ice shelf. Roughness is color-coded and plotted over the MODIS Mosaic Image of Antarctica (Haran et al., 2014). Shown in red is the grounding line for each ice shelf obtained from NASA’s MEaSUREs data-set (Rignot et al., 2013). Also shown in boxes A-H are subsets of each ice shelf, which are shown in greater detail in Figure 2.

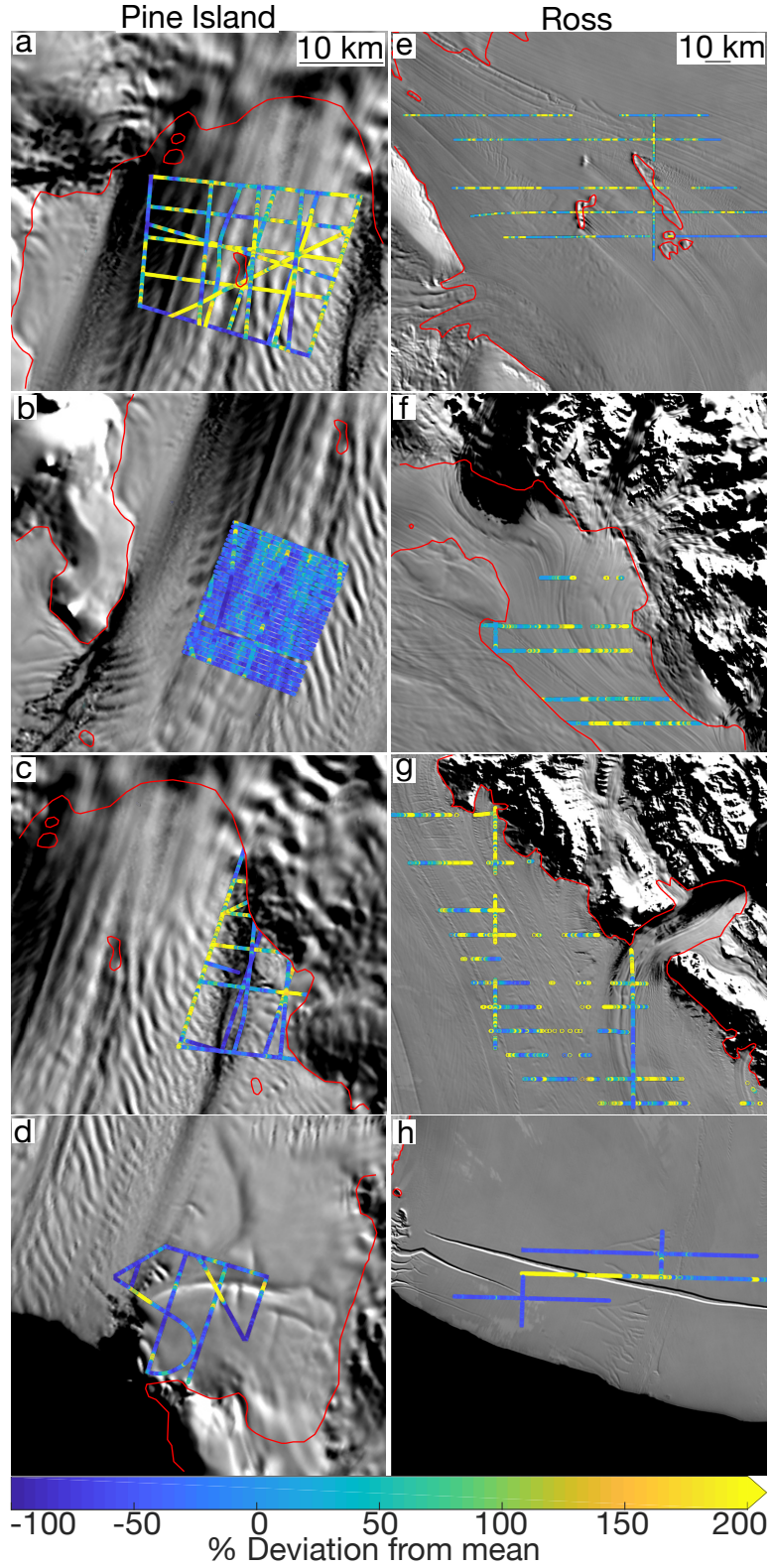


Figure 2. Percent deviation from the mean roughness for Pine Island (left) and Ross ice shelf (right). Panels a and e show pinning points. Panels b and f show melt channels. Panels c and g show shear margins. Panels d and h show rifts.

3.2 Average and spectral characteristics of roughness

We see clear differences in the magnitude of roughness between the Pine Island and Ross ice shelves. Because pinning points, melt channels, crevasses, and rifts elevate roughness, we anticipated that the topography associated with these features would have characteristic spectral signatures. To investigate the spectral characteristics of roughness, we averaged the power spectral density for all the flight tracks over the Pine Island and Ross ice shelves (Figure 3). Contrary to our expectations, we do not see characteristic peaks in the power spectra corresponding to discrete wavelengths. Instead, the spectra for both Pine Island and Ross approximately followed power-laws. Moreover, the power-law exponent is statistically equivalent for both ice shelves, with the primary difference that the spectrum for Pine Island is shifted higher at *all* wavelengths compared to the Ross ice shelf.

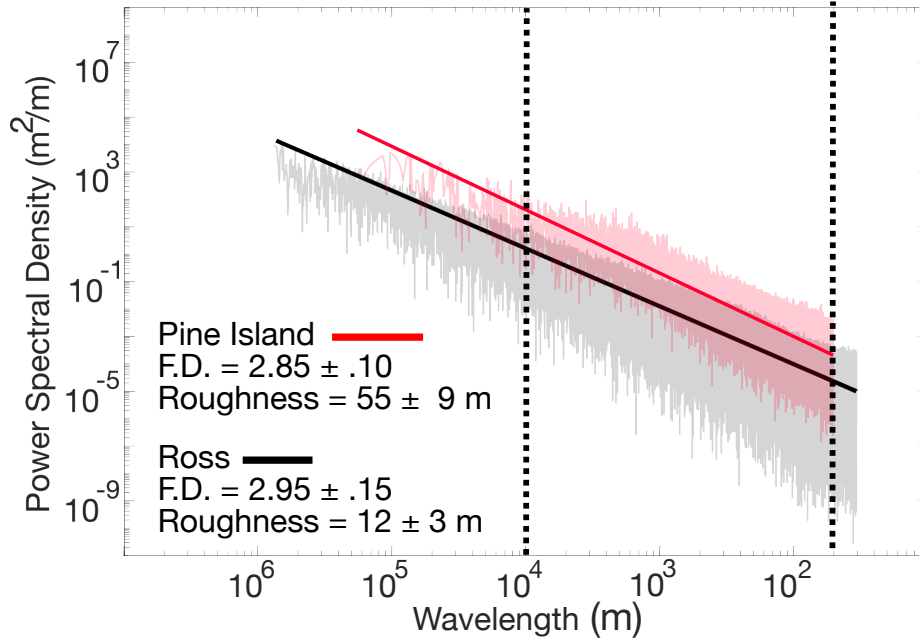


Figure 3. The power spectral density of all tracks going over the Pine Island and Ross ice shelves. Pine Island is plotted in light red and Ross is plotted in light grey. Also shown is a least squares fit of the power-law equation to each spectrum. The solid red line represents the fit for Pine Island while the solid black line represents the fit for Ross. Integration bounds used for calculating the average roughness for each ice shelf are plotted by the black dotted lines.

We also characterized the average roughness for Pine Island and Ross by integrating over the average spectrum of each ice shelf between two wavenumber bounds (dashed lines in Figure 3). We found that the average roughness of Pine Island (55 m) was around five times that of Ross (12 m). This result is consistent with our previous result in Figures 1 and 2, where we showed that roughness was consistently larger on Pine Island than the Ross ice shelf.

The power-law behavior might be a consequence of the fact that tracks intersect with features at different angles, blurring out any characteristic peaks in the spectra. For Pine Island, where tracks are roughly oriented along-flow and transverse-to-flow, we also calculated the average transverse-to-flow roughness and the average longitudinal-to-flow roughness. The transverse-to-flow roughness was about twice as large as the longitudinal to flow roughness (66 m vs 30 m). In both cases however, the spectra of each was approximately power-law with a statistically identical scaling exponent. This indicates that although Pine Island is experiencing increased basal and excavation of melt channels, which are seen mostly in the transverse to flow tracks, the increased roughness is not solely due to the increased prevalence of melt channels. Instead, transverse-to-flow features, like crevasses, are also introducing a larger component of roughness.

3.3 Roughness is highly variable between ice shelves, but the power-law exponent is constant

To determine if these results hold for a larger suite of ice shelves, we next extended our roughness analysis to five other Antarctic ice shelves: Thwaites, Dotson, Getz, Larsen C, and Filchner. We again found that the power-law exponent was statistically identical for all of the ice shelves considered. However, the average roughness varied significantly (Figure 4). Measurements of the average roughness ranged over an order of magnitude, with a high of around 90 m for Thwaites and a low of around 12 m for Ross. However, we do see a pattern with larger roughness associated with ice shelves in the Amundsen Sea Embayment.

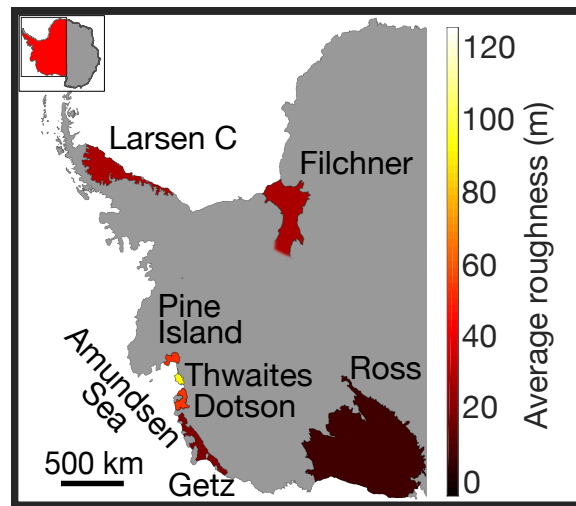


Figure 4. A mapping of roughness across several Antarctic ice shelves. Ice shelves are color coded to match up with the roughness axis

3.4 The average roughness of ice shelves is correlated with basal melt rates

Ice shelves in the Amundsen Sea Embayment have a larger roughness compared to other ice shelves (Figure 4). They also experience much larger basal melt rates due to the intrusion of warm water that happens within the Amundsen Sea (Jenkins et al., 2018; Nakayama et al., 2019). To test for a connection with basal melt, we examined the relationship between the average basal melt rate, obtained from (Liu et al., 2015), and the average roughness of each ice shelf (Figure 5). We see a strong linear trend between increased basal melt and increased roughness. Crucially, this shows that basal melt correlates with—and perhaps triggers—increased roughness of the ice shelves. Intriguingly, based on its apparent power law nature, roughness also appears to increase across a large spectrum of wavelengths, which indicates a complex interplay between increased basal melt and ice dynamics.

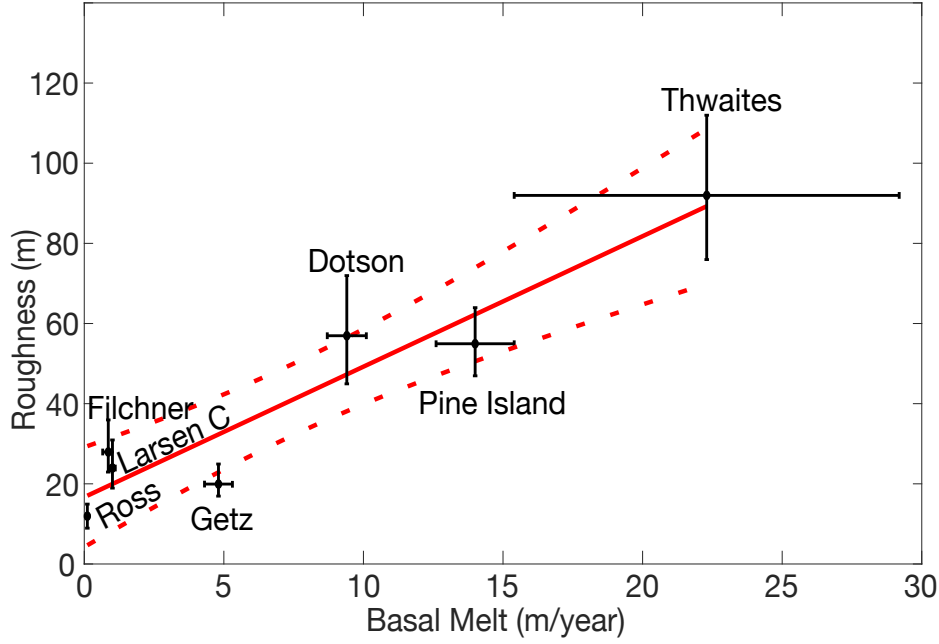


Figure 5. Least squares regression of basal melt and the average roughness of seven Antarctic ice shelves. Plotted in red is the best fit line with 95% confidence bounds

4 Discussion

Our results show a clear relationship between pinning points and roughness. Confining stresses associated with pinning points play a role nucleating crevasses and rifts and are involved in seeding the topographic expressions that eventually become rifts and channels (Still et al., 2018). Our results also show that roughness is increased relative to its *mean* over pinning points and other structural features, with very different roughness associated with these features between ice shelves. This, combined with the connection between roughness and basal melt, suggests basal melt might excavate localized topography, thereby enhancing roughness generated by pinning points and other features. Alternatively, refreezing in colder ocean environments, might fill topographic features, smoothing out the surface. This is similar to the mechanism proposed by (Bassis & Ma, 2015) where increased ocean forcing excavates crevasses resulting in deeper and wider features and is analogous to observations showing marine ice filling suture zones between ice streams (Luckman et al., 2012). This hypothesis, however, contrasts with high resolution two-dimensional models of ice-ocean interaction within crevasses

(Jordan et al., 2014). These models show that the pressure-dependence of the basal melt rate results in lower melt rates or refreezing within crevasses, implying that the ocean will smooth out features. More work is needed to disentangle the mechanisms responsible for the amplification of topography on the 1 m to 100 m scale, including (numerically expensive) three-dimensional models of circulation capable of resolving meter scale features.

Our results also indicate that roughness is strongly correlated with average basal melt rates beneath ice shelves. It is possible that the larger basal melt rates we observe are a direct consequence of the larger roughness. For example, the amount of energy transferred to the ice-ocean interface is often assumed to depend on roughness, albeit on millimeter to centimeter scales (Jenkins et al., 2010). Although the roughness-scale in turbulent energy transfer is much smaller than the scales we consider (and resolve), we also compared point estimates of roughness to basal melt rates (Adusumilli et al., 2020) for Pine Island and found little correlation between local basal melt rates and regions where the local roughness is large. This implies that the interplay between basal melt and roughness is the result of regional rather than localized processes.

Although we are unable to resolve anisotropy or directionality of roughness, increased basal melt appears to be associated with increased roughness across all scales. Instead of finding a strong spectral signature associated with different features, rough ice shelves are rough across a large range of wavelengths. This challenges our classification of features into “basal melt channels” and “crevasses”. Instead, it appears more likely that increased basal melt reduces contact with pinning points and lateral margins, resulting in decreased buttressing that promotes crevassing. At the same time, basal melt channels seed crevasses (Vaughan et al., 2012; Favier et al., 2014) and crevasses may become excavated to become melt channels.

Our observations hint at complex interactions between the ice and ocean over a significant range of scales and features. Critically, however, roughness in ice shelves appears to be not only diagnostic of large basal melt rates, but correlates with ice shelves that are experiencing significant changes, in-

cluding unpinning and grounding line migration (Favier et al., 2014; Milillo et al., 2019). This suggests that increased roughness may be an easily measurable proxy for ice shelf stability. Moreover, increased roughness associated with fracture and failure of ice might point towards future vulnerabilities to ice shelves to collapse through increased fracture and failure. Given that current ice shelf models predict much smoother topography than our observations indicate, we need to better understand the source and evolution of the topographic signature of roughness to better understand these links.

5 Conclusions

We find that roughness varies significantly within and between ice shelves. Pinning points, crevasses, melt channels, and rifts all increase roughness of ice shelves. Additionally, we find that the average roughness of ice shelves has a strong correlation with basal melt, with Amundsen Sea ice shelves that have experienced stark increases in ocean forcing, exhibiting the highest roughness. Moreover, we also find that the average roughness spectra of ice shelves approximately follows a power-law distribution with larger wavelength features having higher magnitude roughness and smaller wavelength features having lower magnitude roughness. These results suggest that ocean forcing is playing a dominant role in the evolution of roughness within and between ice shelves. The reason for this strong connection is less clear, but it hints that we will see continued transitions to rougher ice shelves as more ice shelves are subjected to increased basal melt rates. Crucially, the roughest ice shelves in our study have all experienced grounding line retreat and decreased buttressing, hinting at a direct connection between ocean forcing and the mechanical stability of ice shelves.

Acknowledgments

This work is funded by NASA grant 80NSSC20K0568 and this work is also partially supported by the DOMINOS project, a component of the International Thwaites Glacier Collaboration (ITGC). Support from National Science Foundation (NSF: Grant 1738896) and Natural Environment Re-

search Council (NERC: Grant NE/S006605/1). Logistics provided by NSF-U.S. Antarctic Program and NERC-British Antarctic Survey. Operation Ice-Bridge data sets used in this publication can be found at (<https://nsidc.org/icebridge/portal/map>). BAS data used for Pine Island is found at ([https://secure .antarctica.ac.uk/data/aerogeo/index.php](https://secure.antarctica.ac.uk/data/aerogeo/index.php)). ROSSETTA data used for the Ross ice shelf is found at (<https://pgg.ldeo.columbia.edu/data/rosetta-ice>). Mapping was done with the help of the Antarctic Mapping Toolbox in MATLAB (Greene et al., 2017).

References

- Adusumilli, S., Fricker, H. A., Medley, B., Padman, L., & Siegfried, M. R. (2020, August). Interannual variations in meltwater input to the southern ocean from antarctic ice shelves. *Nature Geoscience*, *13*(9), 616–620. Retrieved from <https://doi.org/10.1038/s41561-020-0616-z> doi: 10.1038/s41561-020-0616-z
- Alley, K. E., Scambos, T. A., Siegfried, M. R., & Fricker, H. A. (2016, March). Impacts of warm water on antarctic ice shelf stability through basal channel formation. *Nature Geoscience*, *9*(4), 290–293. Retrieved from <https://doi.org/10.1038/ngeo2675> doi: 10.1038/ngeo2675
- Bassis, J., & Ma, Y. (2015, January). Evolution of basal crevasses links ice shelf stability to ocean forcing. *Earth and Planetary Science Letters*, *409*, 203–211. Retrieved from <https://doi.org/10.1016/j.epsl.2014.11.003> doi: 10.1016/j.epsl.2014.11.003
- Bell, R., Cordero, I., Das, I., Dhakal, T., Frearson, N., Fricker, H., ... Tinto, K. (2020). *Basal melt, ice thickness and structure of the ross ice shelf using airborne radar data*. U.S. Antarctic Program (USAP) Data Center. Retrieved from <http://www.usap-dc.org/view/dataset/601242> doi: 10.15784/601242
- Clauset, A., Shalizi, C. R., & Newman, M. E. J. (2009, November). Power-law distributions in empirical data. *SIAM Review*, *51*(4), 661–703. Retrieved from <https://doi.org/10.1137/070710111> doi: 10.1137/070710111
- Dixon, D. (2007). *Antarctic mean annual temperature map*. U.S. Antarctic Program Data Center (USAP-DC), via National Snow and Ice Data Center

- (NSIDC). Retrieved from <http://www.usap-dc.org/view/dataset/609318>
doi: 10.7265/N51C1TTV
- Dupont, T. K., & Alley, R. B. (2005, February). Assessment of the importance of ice-shelf buttressing to ice-sheet flow. *Geophysical Research Letters*, 32(4), n/a–n/a. Retrieved from <https://doi.org/10.1029/2004gl022024> doi: 10.1029/2004gl022024
- Dutrieux, P., Stewart, C., Jenkins, A., Nicholls, K. W., Corr, H. F. J., Rignot, E., & Steffen, K. (2014, August). Basal terraces on melting ice shelves. *Geophysical Research Letters*, 41(15), 5506–5513. Retrieved from <https://doi.org/10.1002/2014gl060618> doi: 10.1002/2014gl060618
- Dutrieux, P., Vaughan, D. G., Corr, H. F. J., Jenkins, A., Holland, P. R., Joughin, I., & Fleming, A. H. (2013, September). Pine island glacier ice shelf melt distributed at kilometre scales. *The Cryosphere*, 7(5), 1543–1555. Retrieved from <https://doi.org/10.5194/tc-7-1543-2013> doi: 10.5194/tc-7-1543-2013
- Favier, L., Durand, G., Cornford, S. L., Gudmundsson, G. H., Gagliardini, O., Gillet-Chaulet, F., ... Brocq, A. M. L. (2014, January). Retreat of pine island glacier controlled by marine ice-sheet instability. *Nature Climate Change*, 4(2), 117–121. Retrieved from <https://doi.org/10.1038/nclimate2094> doi: 10.1038/nclimate2094
- Favier, L., Pattyn, F., Berger, S., & Drews, R. (2016, November). Dynamic influence of pinning points on marine ice-sheet stability: a numerical study in dronningmaud land, east antarctica. *The Cryosphere*, 10(6), 2623–2635. Retrieved from <https://doi.org/10.5194/tc-10-2623-2016> doi: 10.5194/tc-10-2623-2016
- Greene, C. A., Gwyther, D. E., & Blankenship, D. D. (2017, July). Antarctic mapping tools for matlab. *Computers & Geosciences*, 104, 151–157. Retrieved from <https://doi.org/10.1016/j.cageo.2016.08.003> doi: 10.1016/j.cageo.2016.08.003
- Gudmundsson, G. H. (2013, April). Ice-shelf buttressing and the stability of marine ice sheets. *The Cryosphere*, 7(2), 647–655. Retrieved from <https://doi.org/10.5194/tc-7-647-2013> doi: 10.5194/tc-7-647-2013
- Haran, T., Bohlander, J., Scambos, T., Painter, T., & Fahnestock, M. (2014). Modis mosaic of antarctica 2008-2009 (moa2009) image map. *Digital media*.
- Jenkins, A., Nicholls, K. W., & Corr, H. F. J. (2010, October). Observation and pa-

- rameterization of ablation at the base of ronne ice shelf, antarctica. *Journal of Physical Oceanography*, 40(10), 2298–2312. Retrieved from <https://doi.org/10.1175/2010jpo4317.1> doi: 10.1175/2010jpo4317.1
- Jenkins, A., Shoosmith, D., Dutrieux, P., Jacobs, S., Kim, T. W., Lee, S. H., ... Stammerjohn, S. (2018, August). West antarctic ice sheet retreat in the amundsen sea driven by decadal oceanic variability. *Nature Geoscience*, 11(10), 733–738. Retrieved from <https://doi.org/10.1038/s41561-018-0207-4> doi: 10.1038/s41561-018-0207-4
- Jeong, S., Howat, I. M., & Bassis, J. N. (2016, November). Accelerated ice shelf rifting and retreat at pine island glacier, west antarctica. *Geophysical Research Letters*, 43(22). Retrieved from <https://doi.org/10.1002/2016gl071360> doi: 10.1002/2016gl071360
- Joe, J., Scaraggi, M., & Barber, J. (2017, July). Effect of fine-scale roughness on the tractions between contacting bodies. *Tribology International*, 111, 52–56. Retrieved from <https://doi.org/10.1016/j.triboint.2017.03.001> doi: 10.1016/j.triboint.2017.03.001
- Jordan, J. R., Holland, P. R., Jenkins, A., Piggott, M. D., & Kimura, S. (2014, February). Modeling ice-ocean interaction in ice-shelf crevasses. *Journal of Geophysical Research: Oceans*, 119(2), 995–1008. Retrieved from <https://doi.org/10.1002/2013jc009208> doi: 10.1002/2013jc009208
- Liu, Y., Moore, J. C., Cheng, X., Gladstone, R. M., Bassis, J. N., Liu, H., ... Hui, F. (2015, March). Ocean-driven thinning enhances iceberg calving and retreat of antarctic ice shelves. *Proceedings of the National Academy of Sciences*, 112(11), 3263–3268. Retrieved from <https://doi.org/10.1073/pnas.1415137112> doi: 10.1073/pnas.1415137112
- Lovejoy, S. (1982, April). Area-perimeter relation for rain and cloud areas. *Science*, 216(4542), 185–187. Retrieved from <https://doi.org/10.1126/science.216.4542.185> doi: 10.1126/science.216.4542.185
- Luckman, A., Jansen, D., Kulesa, B., King, E. C., Sammonds, P., & Benn, D. I. (2012, January). Basal crevasses in larsen c ice shelf and implications for their global abundance. *The Cryosphere*, 6(1), 113–123. Retrieved from <https://doi.org/10.5194/tc-6-113-2012> doi: 10.5194/tc-6-113-2012
- Mandelbrot, B. B., & Wheeler, J. A. (1983, March). The fractal geometry of na-

- ture. *American Journal of Physics*, 51(3), 286–287. Retrieved from <https://doi.org/10.1119/1.13295> doi: 10.1119/1.13295
- McGrath, D., Steffen, K., Scambos, T., Rajaram, H., Casassa, G., & Lagos, J. L. R. (2012). Basal crevasses and associated surface crevassing on the larsen c ice shelf, antarctica, and their role in ice-shelf instability. *Annals of Glaciology*, 53(60), 10–18. Retrieved from <https://doi.org/10.3189/2012aog60a005> doi: 10.3189/2012aog60a005
- Milillo, P., Rignot, E., Rizzoli, P., Scheuchl, B., Mouginot, J., Bueso-Bello, J., & Prats-Iraola, P. (2019, January). Heterogeneous retreat and ice melt of thwaites glacier, west antarctica. *Science Advances*, 5(1), eaau3433. Retrieved from <https://doi.org/10.1126/sciadv.aau3433> doi: 10.1126/sciadv.aau3433
- Nakayama, Y., Manucharyan, G., Zhang, H., Dutrieux, P., Torres, H. S., Klein, P., ... Menemenlis, D. (2019, November). Pathways of ocean heat towards pine island and thwaites grounding lines. *Scientific Reports*, 9(1). Retrieved from <https://doi.org/10.1038/s41598-019-53190-6> doi: 10.1038/s41598-019-53190-6
- Paden, J., Li, J., Leuschen, C., Rodriguez-Morales, F., & Hale, R. (2010). *Icebridge mcds l2 ice thickness, version 1*. NASA National Snow and Ice Data Center Distributed Active Archive Center. Retrieved from <https://doi.org/10.5067/gdq0cucvte2q> doi: 10.5067/gdq0cucvte2q
- Pritchard, H. D., Ligtenberg, S. R. M., Fricker, H. A., Vaughan, D. G., van den Broeke, M. R., & Padman, L. (2012, April). Antarctic ice-sheet loss driven by basal melting of ice shelves. *Nature*, 484(7395), 502–505. Retrieved from <https://doi.org/10.1038/nature10968> doi: 10.1038/nature10968
- Rignot, E. (2004). Accelerated ice discharge from the antarctic peninsula following the collapse of larsen b ice shelf. *Geophysical Research Letters*, 31(18). Retrieved from <https://doi.org/10.1029/2004gl020697> doi: 10.1029/2004gl020697
- Rignot, E., Jacobs, S., Mouginot, J., & Scheuchl, B. (2013, June). Ice-shelf melting around antarctica. *Science*, 341(6143), 266–270. Retrieved from <https://doi.org/10.1126/science.1235798> doi: 10.1126/science.1235798
- Rignot, E., Mouginot, J., Scheuchl, B., van den Broeke, M., van Wessem, M. J., &

- 445 Morlighem, M. (2019, jan). Four decades of antarctic ice sheet mass balance
 446 from 1979–2017. *Proceedings of the National Academy of Sciences*, 116(4),
 447 1095–1103. Retrieved from <https://doi.org/10.1073/2Fpnas.1812883116>
 448 doi: 10.1073/pnas.1812883116
- 449 Robel, A. A., & Banwell, A. F. (2019, November). A speed limit on ice shelf col-
 450 lapse through hydrofracture. *Geophysical Research Letters*, 46(21), 12092–
 451 12100. Retrieved from <https://doi.org/10.1029/2019gl084397> doi:
 452 10.1029/2019gl084397
- 453 Rott, H., Skvarca, P., & Nagler, T. (1996, February). Rapid collapse of
 454 northern larsen ice shelf, antarctica. *Science*, 271(5250), 788–792. Re-
 455 trieved from <https://doi.org/10.1126/science.271.5250.788> doi:
 456 10.1126/science.271.5250.788
- 457 Scambos, T., Hulbe, C., & Fahnestock, M. (2003, April). Climate-induced ice shelf
 458 disintegration in the antarctic peninsula. In *Antarctic peninsula climate vari-*
 459 *ability: Historical and paleoenvironmental perspectives* (pp. 79–92). American
 460 Geophysical Union. Retrieved from <https://doi.org/10.1029/ar079p0079>
 461 doi: 10.1029/ar079p0079
- 462 Shean, D. E., Joughin, I. R., Dutrieux, P., Smith, B. E., & Berthier, E. (2019, Octo-
 463 ber). Ice shelf basal melt rates from a high-resolution digital elevation model
 464 (DEM) record for pine island glacier, antarctica. *The Cryosphere*, 13(10),
 465 2633–2656. Retrieved from <https://doi.org/10.5194/tc-13-2633-2019>
 466 doi: 10.5194/tc-13-2633-2019
- 467 Shepherd, A., Fricker, H. A., & Farrell, S. L. (2018, June). Trends and con-
 468 nections across the antarctic cryosphere. *Nature*, 558(7709), 223–232.
 469 Retrieved from <https://doi.org/10.1038/s41586-018-0171-6> doi:
 470 10.1038/s41586-018-0171-6
- 471 Sifuzzaman, M. (2009). Application of wavelet transform and its advantages com-
 472 pared to fourier transform..
- 473 Still, H., Campbell, A., & Hulbe, C. (2018, December). Mechanical analysis of pin-
 474 ning points in the ross ice shelf, antarctica. *Annals of Glaciology*, 60(78), 32–
 475 41. Retrieved from <https://doi.org/10.1017/aog.2018.31> doi: 10.1017/
 476 aog.2018.31
- 477 Vaughan, D. G., Corr, H. F. J., Bindshadler, R. A., Dutrieux, P., Gudmundsson,

- 478 G. H., Jenkins, A., ... Wingham, D. J. (2012, August). Subglacial melt chan-
 479 nels and fracture in the floating part of pine island glacier, antarctica. *Journal*
 480 *of Geophysical Research: Earth Surface*, 117(F3), n/a–n/a. Retrieved from
 481 <https://doi.org/10.1029/2012jff002360> doi: 10.1029/2012jff002360
- 482 Webber, B. G. M., Heywood, K. J., Stevens, D. P., Dutrieux, P., Abrahamsen,
 483 E. P., Jenkins, A., ... Kim, T. W. (2017, February). Mechanisms driving
 484 variability in the ocean forcing of pine island glacier. *Nature Communica-*
 485 *tions*, 8(1). Retrieved from <https://doi.org/10.1038/ncomms14507> doi:
 486 10.1038/ncomms14507
- 487 Werner, M., Jouzel, J., Masson-Delmotte, V., & Lohmann, G. (2018, August).
 488 Reconciling glacial antarctic water stable isotopes with ice sheet topogra-
 489 phy and the isotopic paleothermometer. *Nature Communications*, 9(1).
 490 Retrieved from <https://doi.org/10.1038/s41467-018-05430-y> doi:
 491 10.1038/s41467-018-05430-y
- 492 Whitehouse, D. J. (2004). *Surfaces and their measurement*. Kogan Page Science.